Electronic Supplementary Material (ESI) for Nanoscale.

Effect of Terminal Groups on the Degradation Stability of $Ti_3C_2T_z$ MXenes

Swarnima Athavale[1], Stefano A. Micci-Barreca[1], Kailash Arole[2], Vrushali Kotasthane[2], Jodie L. Lutkenhaus[1,2], Miladin Radovic[2], Micah J. Green[1,2]*

[1]Artie McFerrin Department of Chemical Engineering, Texas A&M University, College Station, TX 77843, USA

[2]Department of Materials Science and Engineering, Texas A&M University, College Station, TX 77843, USA

*Corresponding author: micah.green@tamu.edu

Supplementary Information

Table S1. Elemental composition of (a) $CdBr_2$ etched ML-$Ti_3C_2T_z$ on day 0 vs day 21; (b) $CdCl_2$ etched ML- $Ti_3C_2T_z$ on day 0 vs day 21

a

Elements	**Day 0**	**Day 21**
-	**wt.%**	**wt.%**
C	32.8	10.7
Ti	31.9	43.0
Br	23.3	2.3
O	11.3	43.2
Al	0.6	0.8

b

Elements	**Day 0**	**Day 21**
-	**wt.%**	**wt.%**
C	34.5	31.8
Ti	40.5	23.8
Cl	16.7	2.8
O	7.8	40.7
Al	0.6	0.9

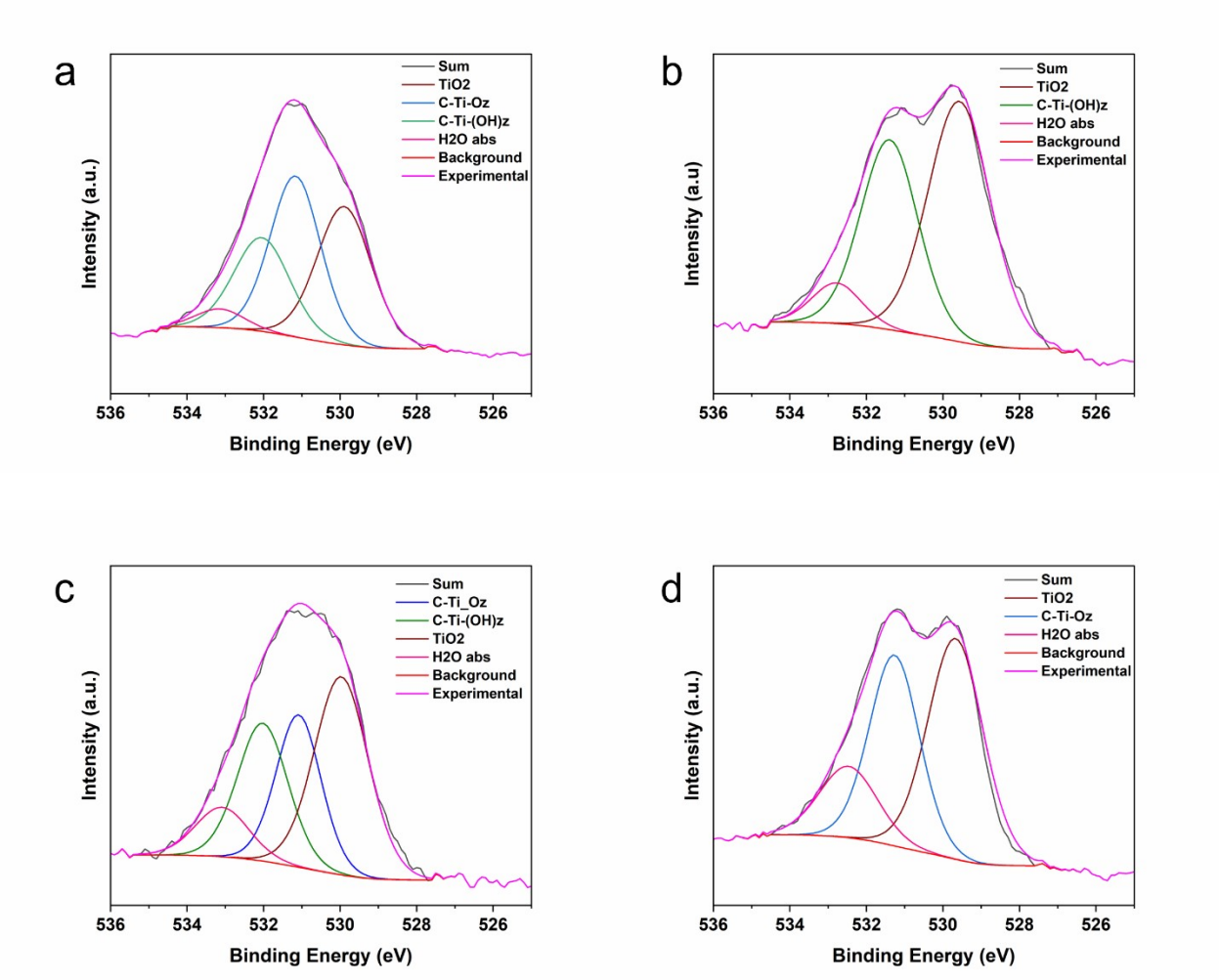

Figure S1. Deconvoluted O 1s X-ray photoelectron spectroscopy (XPS) of (a) $CdBr_2$ etched ML-$Ti_3C_2T_z$ on day 0; (b) $CdBr_2$ etched ML- $Ti_3C_2T_z$ after 21 days of degradation; (c) $CdCl_2$ etched ML- $Ti_3C_2T_z$ on day 0; (d) $CdCl_2$ etched ML- $Ti_3C_2T_z$ after 21 days of degradation.

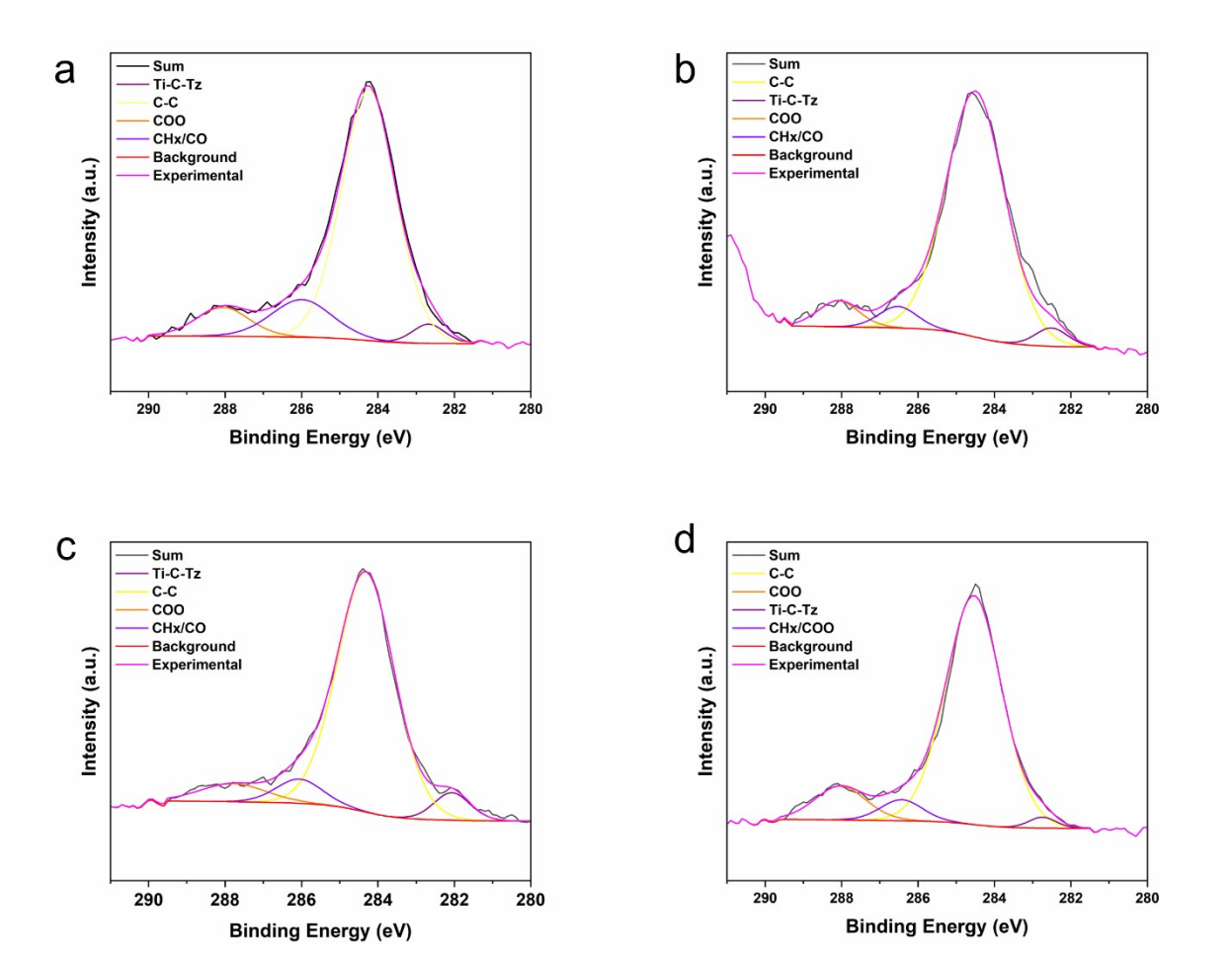

Figure S2. Deconvoluted C 1s X-ray photoelectron spectroscopy (XPS) of (a) $CdBr_2$ etched ML-$Ti_3C_2T_z$ on day 0; (b) $CdBr_2$ etched ML- $Ti_3C_2T_z$ after 21 days of degradation; (c) $CdCl_2$ etched ML- $Ti_3C_2T_z$ on day 0; (d) $CdCl_2$ etched ML- $Ti_3C_2T_z$ after 21 days of degradation.

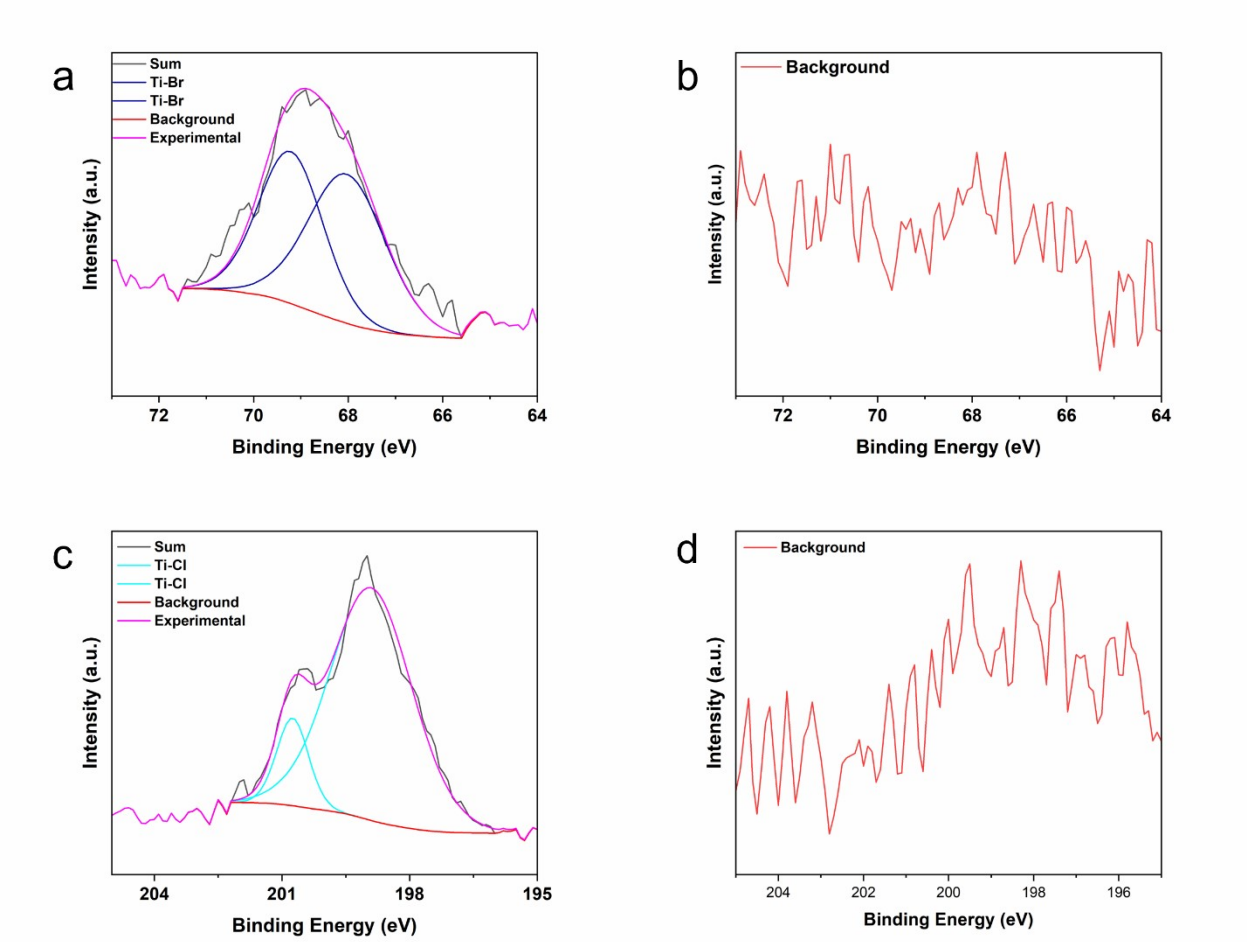

Figure S3. Deconvoluted Br 3d X-ray photoelectron spectroscopy (XPS) of (a) $CdBr_2$ etched ML-$Ti_3C_2T_z$ on day 0; (b) $CdBr_2$ etched ML-$Ti_3C_2T_z$ after 21 days of degradation; Deconvoluted Cl 2p X-ray photoelectron spectroscopy (XPS) of (c) $CdCl_2$ etched ML-$Ti_3C_2T_z$ on day 0; (d) $CdCl_2$ etched ML-$Ti_3C_2T_z$ after 21 days of degradation.

Section S1. XPS analysis

XPS analysis was done on the ML-$Ti_3C_2T_z$ powders on days 0 and 21 after synthesis using an Omicron XPS/UPS with an Argus detector. Samples were stored in a vacuum chamber at room temperature prior to analysis. First, high-resolution Ti 2p, O 1s, C 1s, Br 3d (in the case of $CdBr_2$ etched ML-$Ti_3C_2T_z$) and Cl 2p (in the case of $CdCl_2$ etched ML- $Ti_3C_2T_z$) region spectra were collected, followed by peak convolution using the Casa XPS software. The peak-fitting procedure was done as per known peak positions reported in literature using the Gaussian-Lorentzian line shapes and a few constraints.[1-3] The binding energies of all the component

peak positions were constrained to ± 0.5 eV of the initial values. Moreover, the full width at half maximum (FWHM) of the component peaks were also constrained to approximately match values reported in literature. In the case of the Ti 2p region, component peaks associated with MXenes were fit using asymmetric Gaussian-Lorentzian line shapes. Furthermore, the area ratio of the Ti $2p_{3/2}$ and the Ti $2p_{1/2}$ peaks was constrained to 2:1. Additionally, the difference between the Ti $2p_{3/2}$ and the Ti $2p_{1/2}$ peak positions for each component was also constrained to 6.1 eV (for MXene related peaks) and 5.6 eV (for TiO_2 peaks), as reported in the literature.[2] **Table S2** summarizes the component % areas obtained from the peak deconvolutions of the Ti 2p region for $CdCl_2$ and $CdBr_2$ etched ML-$Ti_3C_2T_z$, respectively.

Component	**Peak positions (eV)**	**% areas of components from Ti 2p region (%)**			
		$CdBr_2$ etched ML-$Ti_3C_2T_z$		**$CdCl_2$ etched ML- $Ti_3C_2T_z$**	
		Day 0	**Day 21**	**Day 0**	**Day 21**
	2p3/2(2p1/2)	**2p3/2 (2p1/2)**	**2p3/2 (2p1/2)**	**2p3/2 (2p1/2)**	**2p3/2 (2p1/2)**
Ti-C	454.9 (460.9)	19.7 (9.9)	0 (0)	17.4 (8.7)	0(0)
Ti^{+2}	455.9 (461.4)	10.6 (5.3)	4.2 (2.1)	11 (5.5)	0 (0)
Ti^{+3}	457.1 (462.6)	11.8(5.9)	0 (0)	7.4 (3.7)	3.3 (1.65)
TiO_2	458.5 (464.1)	24.6 (12.3)	62.5 (31.25)	30.9 (15.45)	63.4 (31.7)
% change in TiO_2 from day 0 to day 21 (%)		154		105	

Table S2. % areas of different Ti 2p region component pairs from (a) $CdBr_2$ etched ML-$Ti_3C_2T_z$ on day 0 vs day 21; (b) $CdCl_2$ etched ML- $Ti_3C_2T_z$ on day 0 vs day 21

Table S3. Summary of the bond dissociation energies for M-O and M-X bonds, taken from Refs [4, 5]

Bond	Bond dissociation energy at 298 K (kJ/mol)
Ti-O	666.5
Ti-F	569.0
Ti-Cl	405.4
Ti-Br	373.0

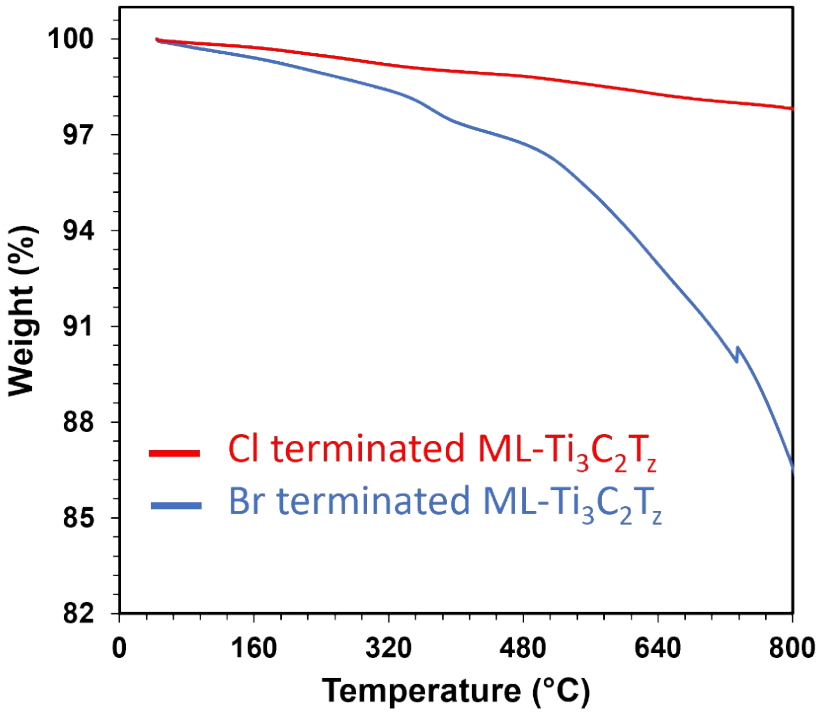

Figure S4. Thermogravimetric analysis of Br and Cl terminated ML-$Ti_3C_2T_z$ indicating the higher thermal stability of Cl terminated MXene compared to Br terminated.

References

[1] X. Zhao, A. Vashisth, E. Prehn, W. Sun, S.A. Shah, T. Habib, Y. Chen, Z. Tan, J.L. Lutkenhaus, M. Radovic, Antioxidants unlock shelf-stable Ti3C2Tx (MXene) nanosheet dispersions, Matter 1(2) (2019) 513-526.
[2] V. Natu, M. Benchakar, C. Canaff, A. Habrioux, S. Celerier, M.W. Barsoum, A critical analysis of the X-ray photoelectron spectra of Ti3C2Tz MXenes, Matter 4(4) (2021) 1224-1251.
[3] M. Li, J. Lu, K. Luo, Y. Li, K. Chang, K. Chen, J. Zhou, J. Rosen, L. Hultman, P. Eklund, Element replacement approach by reaction with Lewis acidic molten salts to synthesize nanolaminated MAX phases and MXenes, Journal of the American Chemical Society 141(11) (2019) 4730-4737.
[4] V. Kamysbayev, S. Filatov Alexander, H. Hu, X. Rui, F. Lagunas, D. Wang, F. Klie Robert, V. Talapin Dmitri, Covalent surface modifications and superconductivity of two-dimensional metal carbide MXenes, Science 369(6506) (2020) 979-983.
[5] Y.-R. Luo, Comprehensive handbook of chemical bond energies, CRC press2007.